

MEASUREMENT OF PARTICLE VELOCITY IN A TWO-PHASE JET BY DOUBLE-EXPOSURE SPECKLE PHOTOGRAPHY

O. V. Achasov, O. G. Penyaz'kov, and
F. Fisson

UDC 621.374

Double-exposure speckle photography was used to measure the instantaneous particle velocity field in an intense high-velocity two-phase jet.

Introduction. Measurement of particle velocities in two-phase jets flowing out of nozzles has been the object of many theoretical and experimental studies. However, not as much information has been obtained so far about the instantaneous distribution of the velocity field [1]. The efforts of many authors were mainly made to measure local velocities on the periphery of a two-phase jet with a particle concentration and size sufficient for using laser Doppler velocity meters (LDVM) [2, 3]. Meanwhile, LDVM and thermoanemometers give instantaneous components of particle velocities only at one point of the flow, and point-by-point scanning over the entire flow is necessary to obtain the whole information about the distribution of the average velocity and its fluctuations in a two-phase jet. It should be noted that this scanning does not provide the instantaneous distribution of the velocity field over the whole jet at any time. Consequently, this experimental equipment only provides qualitative information about the velocity over the whole flow field.

In the present work the method of double-exposure speckle photography (SP) [4-6] is used to measure the instantaneous particle velocity field in an intense high-velocity two-phase jet. Double-exposure speckle photography is a two-stage process. In the first stage particles are photographed in the flow. During the first pulse of laser illumination, positions of particles located inside the laser sheet are stored on a film. The particles move during the time between the first and second exposures, and at the time of the second pulse of laser illumination their new positions are stored on the same film. In the second stage processing and analysis of the obtained double-exposure photograph (specklegram) are carried out to isolate information about the velocity field. The photograph is developed and copied by the contact method to obtain a positive image of every particle in the flow. Then, the resultant positive is placed in the scheme of reconstructing the specklegram for analysis of the Young interference bands since each pair of displaced particles functions under illumination as a light source in a Young interferometer [7].

Experimental Setup and Specklegram Reconstruction Scheme. An intense high-velocity two-phase jet flowing out of a nozzle was used as the object of the study. A high-power neodymium laser with a frequency duplication system was used for illumination. The wavelength of the output laser beam was $\lambda = 535$ nm. The laser sheet for illumination of the jet was formed when the laser beam passed through cylindrical and spherical lenses. The latter was used for decreasing the thickness and divergence of the laser sheet. For uniform illumination of water drops in the cross section measured, use was made of a spherical mirror that was located at twice the focal length from the focal plane of the spherical lens and reflected the laser beam in the opposite direction. The length of the laser illumination pulses was $\Delta\tau = 30$ nsec. The delay between successive illumination pulses depended on the velocity of the jet and could be varied from 10 nsec to 10 sec.

The measuring cross section started at 3 cm from the nozzle exit section in the downstream direction and had a size of 50×50 mm. For reduction of the effect of secondary scattering, the longest possible distance was

Scientific Academic Complex "A. V. Luikov Heat and Mass Transfer Institute, Academy of Sciences of Belarus," Minsk, Belarus. Translated from *Inzhenerno-Fizicheskii Zhurnal*, Vol. 69, No. 2, pp. 224-229, March-April, 1996. Original article submitted March 9, 1995.

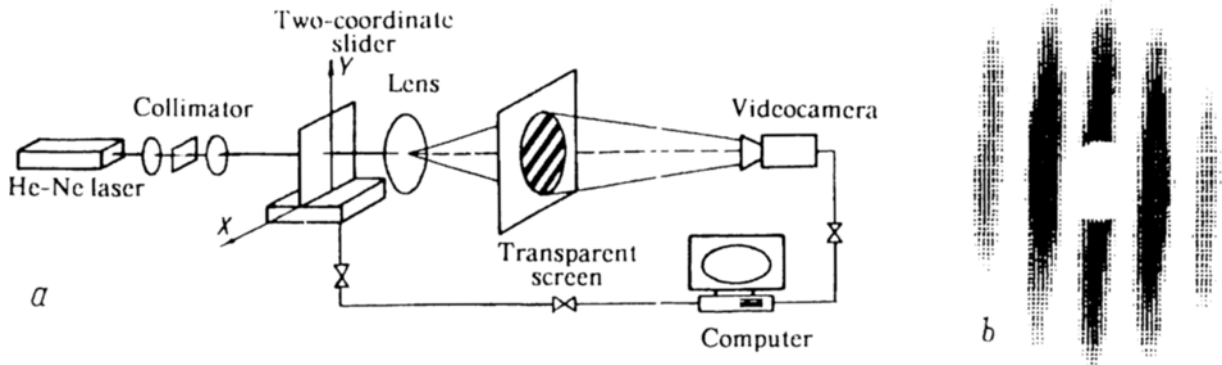


Fig. 1. Optical scheme for analysis of Young bands (a) and a typical form of interference bands (b) behind the twice exposed image of a two-phase water jet.

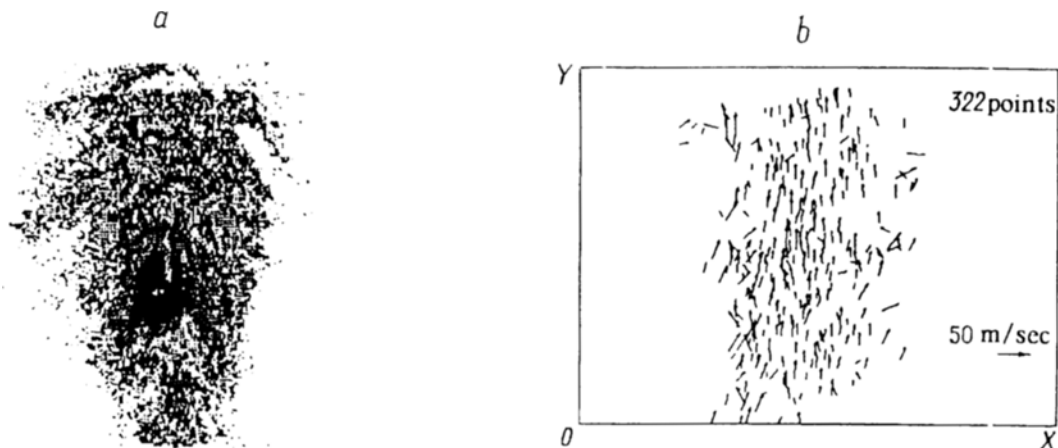


Fig. 2. A typical photograph of the two-phase jet studied (a) and the corresponding instantaneous particle velocity field (b).

chosen between the photocamera and the water jet, and the lens stop was the minimum. In Fig. 1a the optical scheme is shown for analysis of the Young bands behind the doubly exposed image of the two-phase water jet. An He-Ne laser was used as the light source. The laser beam passed through a collimator, which decreased the beam divergence and allowed variation of the beam diameter. The specklegram was fixed in a two-coordinate slider for subsequent scanning. The Young interference bands from displaced water drops were formed by a lens for Fourier transformation on a transparent screen. The images of the interference bands were input into a PC by a videocamera mounted behind the screen. A typical form of the Young interference bands obtained is shown in Fig. 1b. A special computer program for processing the images was used to calculate the distance between the interference bands δ and the angle α of their slope to the X axis, which are related to the vector of displacement of the water drops in the time between two specklegram exposures by the relation

$$\Delta = L\lambda/\delta. \quad (1)$$

where λ is the wavelength of the He-Ne laser, L is the focal length of the lens for the Fourier transformation. For the components of the velocity vector of the drops we have

$$\begin{aligned} V_x &= L\lambda \sin \alpha / \delta t, \\ V_y &= L\lambda \cos \alpha / \delta t, \end{aligned} \quad (2)$$

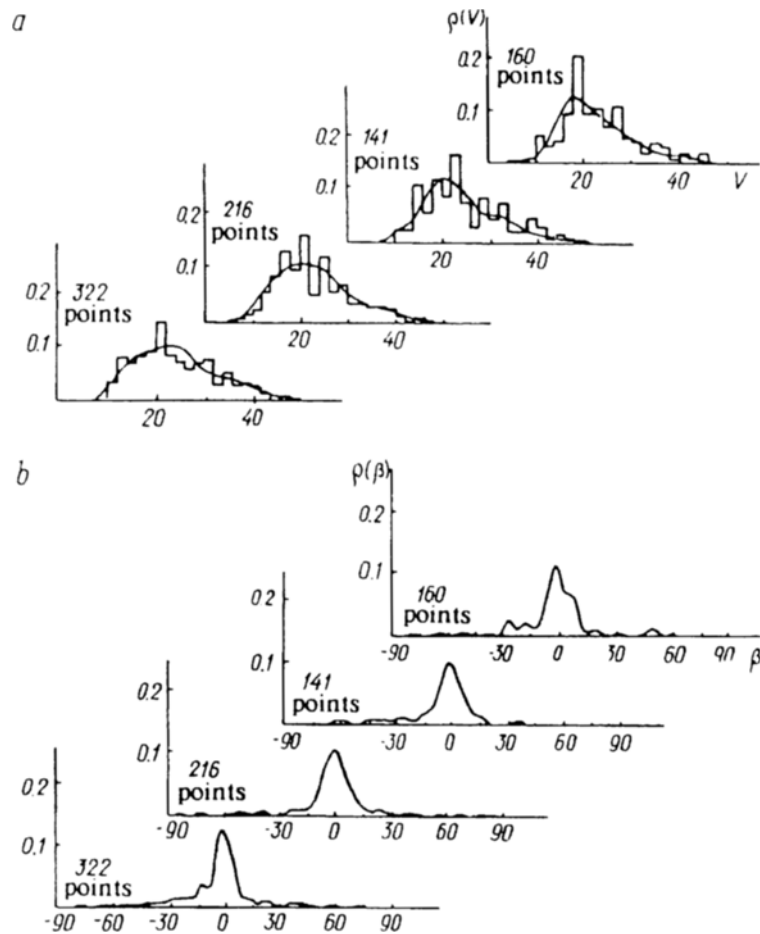


Fig. 3. Probability density functions for the particle velocity (a) and the angle of slope of the velocity vector to the Y axis (b) obtained from speckle photography measurements of the velocity field for four instantaneous realizations of the flow in a two-phase jet.

where t is the time between two exposures.

In our experiments the accuracy of measuring the particle velocity was determined by the error in calculating the slope angle and the distance between the Young interference bands and amounted to 3%.

Experimental Results. In Fig. 2 one can see a typical photograph of the investigated water jet flowing out of a nozzle into a medium with an ambient-air pressure of 1 atm and the corresponding instantaneous particle velocity field measured by the method of double-exposure speckle photography. As can be seen from the figure, the jet consists of a dense central core containing virtually undecomposed water clusters and clouds of dilute water drops that surround the core of the jet on the periphery. According to the microscope measurements taken, in the recording cross section the jet consists of water drops whose size varies from 70 to 400 μm .

Fundamental experimental problems arose in the stage of analysis of the specklogram sections corresponding to the sites with the highest concentration of water drops, since the image of each particle creates an interference pattern with any other particle located in the region of the light beam of the reconstructing He-Ne laser. This results in mixing of the Young interference bands since in many cases, even in such a small flow region, water drops have different sizes and velocities, and as a result, it is impossible to use the numerical procedure for computer analysis of interference bands. In order to exclude the effect of parasitic interference, the diameter of the beam from the reconstructing laser was changed to 0.5 mm and the displacement of the particle images between two exposures was simultaneously decreased by varying the time interval between two pulses of the laser illumination. In our experiments this interval was $t = 10 \mu\text{sec}$. Meanwhile, to measure the velocity of water drops

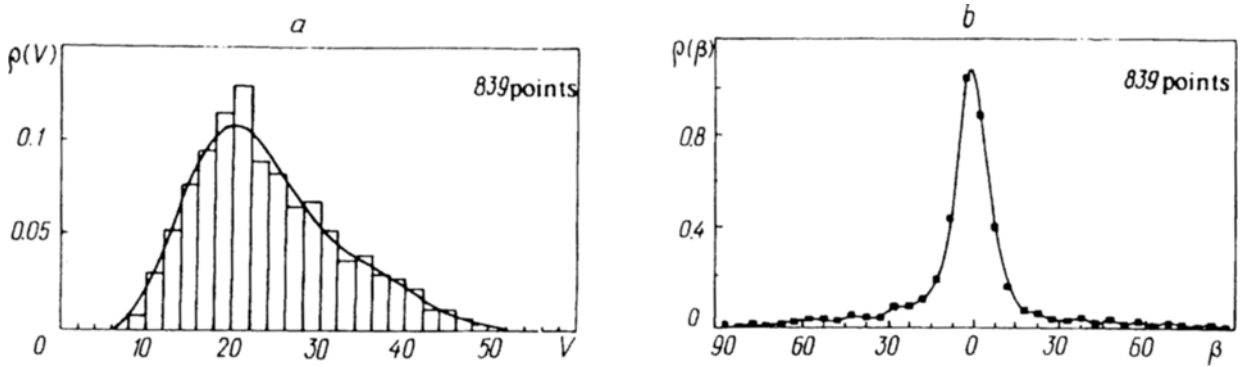


Fig. 4. Complete distribution functions for the velocity (a) and the angle of slope of the velocity vector to the Y axis (b) for four instantaneous realizations of the flow in a two-phase jet.

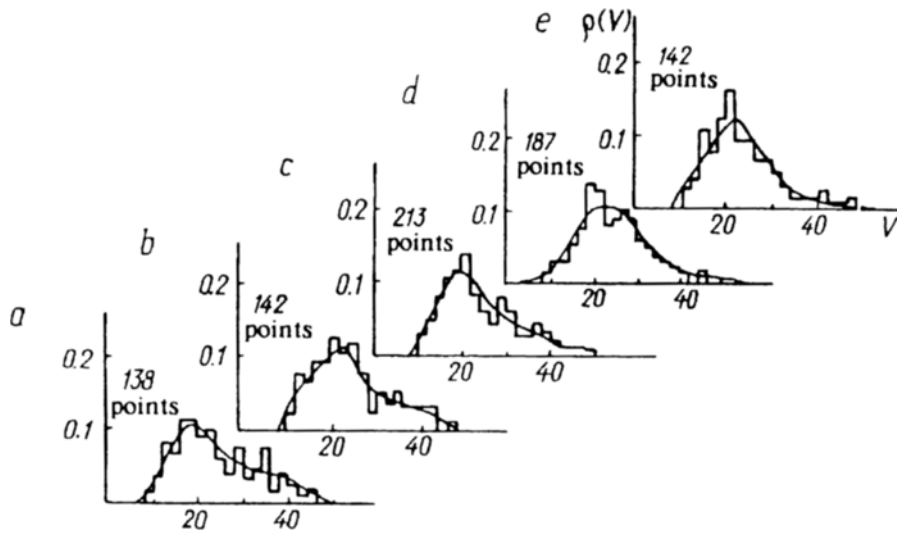


Fig. 5. Evolution of the probability density function for the particle velocity with increase in the distance from the nozzle exit section: a) $Y = 0-9$ mm; b) $9-18$; c) $27-36$; e) $36-45$.

whose size is comparable with the diameter of the reconstructing He-Ne laser beam, the photocamera was artificially diaphragmed, because of which the size of the particle images on the specklegram could be diminished. Nevertheless in some of the most dense areas of the two-phase water jet it was not possible to use the procedure for analysis of the Young bands.

Probability density functions (PDF) for the velocity and the angle of the velocity vector to the Y axis are presented in Fig. 3. The PDF were calculated over the whole flow region. In Fig. 4 one can see complete distribution functions for the velocity and the angle of slope of the velocity vector to the Y axis. As can be seen from Fig. 4a, the form of the complete PDF differs substantially from the normal one in the region of high velocities. This can be explained by the fact that the particle velocity field was measured in the initial section of the jet, in which disintegration and collision of water drops were important for the flow organization. The complete PDF for the velocity can be expressed as a superposition of two normal distribution functions corresponding to the average velocities $\bar{V}_1 \approx 20$ m/sec and $\bar{V}_2 \approx 34$ m/sec. It is evident that as the distance from the nozzle exit section increases, the form of the complete PDF should approach the normal one. This fact is a good illustration of evolution of the distribution functions constructed for different cross sections of the two-phase jet along the flow (Fig. 5). As can be seen from Fig. 5, in the region of high velocities the "tail" of the PDF gradually vanishes with increase in the distance along the Y axis.

Conclusion. The method of double-exposure speckle photography is used effectively for measuring the instantaneous particle velocity field in a high-velocity two-phase jet flowing out of a nozzle. With the method suggested, the complete probability distribution function is found for the velocity and the angle of slope of the velocity vector to the jet axis. The complete distribution function constructed for several instantaneous realizations of the flow field not only determines the averaged characteristics of particle motion in the jet but also allows the researcher to follow the evolution of the particles as the distance from the nozzle exit section increases. The method gives satisfactory results even in the case of velocity measurements in the most dense regions of the jet core and for particles having substantially different sizes.

NOTATION

λ , wavelength of laser radiation; Δt , duration of laser pulse; δ , distance between Young interference bands; α , angle of slope of interference bands to X axis; Δ , displacement of particle image in the time between two exposures; L , focal length of the lens for Fourier transformation; V , particle velocity; V_x, Y_y , values of projections of particle velocity vector onto the coordinate axes; t , time interval between two laser pulses; $\rho(V)$, probability density function for particle velocity; β , angle of slope of velocity vector to Y ; $\rho(\beta)$, probability density function for the angle of slope of velocity vector to Y axis.

REFERENCES

1. N. A. Chieger and C. G. McCreath, *Acta Astronautica*, No. 1, 687-710 (1974).
2. M. Maeda and K. Hishida, in: *Laser Diagnostics and Modeling of Combustion*, Springer-Verlag, Berlin (1987), pp. 1-10.
3. G. Gouesbet and M. Ledoux, *Opt. Eng.*, 23, No. 5, 631-636 (1984).
4. D. B. Barker and M. E. Fourney, *Fluid Mech.*, 16, No. 6, 209-214 (1976).
5. R. Meynart, *Appl. Opt.* 22, No. 4, 535-540 (1983).
6. R. J. Adrian, *Proc. 3rd Int. Symp. on Application of Laser Velocimetry to Fluid Mechanics*, Lisbon (1986).
7. J. M. Bursh and J. M. J. Tokarski, *Optica Acta*, 15, No. 2, 101-111 (1986).